OPEN ACCESS Freely available online

PLoS one

Regeneration of the Exocrine Pancreas Is Delayed in Telomere-Dysfunctional Mice

Guido von Figura[1,2], Martin Wagner[2], Kodandaramireddy Nalapareddy[1], Daniel Hartmann[1,3], Alexander Kleger[1,2], Luis Miguel Guachalla[1], Harshvardhan Rolyan[1], Guido Adler[2], Karl Lenhard Rudolph[1]*

1 Institute of Molecular Medicine and Max-Planck-Research-Group on Stem Cell Aging, University of Ulm, Ulm, Germany, **2** Department of Internal Medicine I, University of Ulm, Ulm, Germany, **3** Department of Surgery, Technical University of Munich, Munich, Germany

Abstract

Introduction: Telomere shortening is a cell-intrinsic mechanism that limits cell proliferation by induction of DNA damage responses resulting either in apoptosis or cellular senescence. Shortening of telomeres has been shown to occur during human aging and in chronic diseases that accelerate cell turnover, such as chronic hepatitis. Telomere shortening can limit organ homeostasis and regeneration in response to injury. Whether the same holds true for pancreas regeneration in response to injury is not known.

Methods: In the present study, pancreatic regeneration after acute cerulein-induced pancreatitis was studied in late generation telomerase knockout mice with short telomeres compared to telomerase wild-type mice with long telomeres.

Results: Late generation telomerase knockout mice exhibited impaired exocrine pancreatic regeneration after acute pancreatitis as seen by persistence of metaplastic acinar cells and markedly reduced proliferation. The expression levels of p53 and p21 were not significantly increased in regenerating pancreas of late generation telomerase knockout mice compared to wild-type mice.

Conclusion: Our results indicate that pancreatic regeneration is limited in the context of telomere dysfunction without evidence for p53 checkpoint activation.

Citation: von Figura G, Wagner M, Nalapareddy K, Hartmann D, Kleger A, et al. (2011) Regeneration of the Exocrine Pancreas Is Delayed in Telomere-Dysfunctional Mice. PLoS ONE 6(2): e17122. doi:10.1371/journal.pone.0017122

Editor: Ben Ko, Chinese University of Hong Kong, Hong Kong

Received October 23, 2010; **Accepted** January 2, 2011; **Published** February 22, 2011

Funding: Funding was provided by Deutsche Forschungsgemeinschaft (SFB518). The funder had no role in study design, data collection and analysis, decision to publish, or preparation of the manuscript.

Competing Interests: The authors have declared that no competing interests exist.

* E-mail: lenhard.rudolph@uni-ulm.de

Introduction

Telomeres represent tandem repeat sequences at the end of the chromosomes that protect chromosomes against DNA degradation, fusions, and induction of chromosomal instability. Telomeres shorten with each round of cell division due to the 'end-replication-problem' of the DNA polymerase [1]. Upon reaching a critical length, telomere dysfunction induces an activation of the p53-checkpoint, which, in turn, results in either apoptosis or p21-dependent cellular senescence [2–5]. The enzyme telomerase is able to prevent telomere shortening by de-novo synthesis of the telomere sequence. In humans, telomerase is active in germ cells, during embryogenesis, and, to some extent, in adult stem cells.

Impaired organ maintenance and regeneration are hallmarks of aging. On the molecular level, telomere shortening occurs in most human tissues during aging [6]. To what extent it causally contributes to aging in humans is still under debate. In addition, telomere shortening has been linked to various chronic diseases, such as anemia, chronic infections, Alzheimer's disease, and chronic liver disease [6]. Mutations in telomerase are the cause of dyskeratosis congenita and have also been found in pulmonary fibrosis and aplastic anemia patients [7,8]. Telomere shortening has also been linked to the progression of chronic liver disease, especially with the formation of cirrhosis in response to chronic hepatitis [9]. Taken together, these findings indicate that telomere shortening is involved in the pathogenesis of chronic diseases and may limit organ regeneration.

In order to analyze the consequences of telomere dysfunction *in vivo*, we made use of the telomerase knockout ($mTerc^{-/-}$) mouse [10,11]. $mTerc^{-/-}$ mice are lacking the RNA component of telomerase, which leads to an abrogation of the ability to elongate telomeres during cell division. These mice are characterized by continuous telomere shortening with successive generations. As a consequence, late generation $mTerc^{-/-}$ mice show a progeroid phenotype with impaired maintenance of highly proliferative organs, such as the intestinal epithelium and the hematopoetic system [11]. In addition, studies on $mTerc^{-/-}$ mice have revealed that telomere shortening limits liver regeneration upon acute or chronic injury [12,13].

It is currently unknown whether telomere shortening would impair the regenerative capacity of the pancreas. Pancreas regeneration itself is crucial in response to acute or chronic pancreatitis since both processes damage tissue integrity. It has been shown that acute pancreatitis has a more unfavourable

outcome in aged compared to young patients [14]. In addition, it is known that successive telomere shortening occurs in the human pancreas during aging [15]. However, the effect of age and the potential contributions of telomere shortening to pancreatic regeneration after acute pancreatitis have not yet been investigated.

In the present study, we used a late generation telomerase knockout mouse model (G3 mTerc$^{-/-}$) in order to study consequences of telomere shortening on pancreas regeneration after cerulein-induced acute pancreatitis. In this model, repetitive cerulein injections lead to an acute inflammation with significant damage predominantly to the exocrine pancreas followed by successive complete regeneration [16]. This study provides the first experimental evidence that telomere shortening impairs regeneration of the exocrine pancreas.

Results

Normal pancreas development of telomerase knockout mice despite telomere shortening

Aged telomerase knockout mice are characterized by an impairment in the maintenance of highly proliferative organs leading to intestine and bone marrow failure [11]. An analysis of histological sections revealed no morphologic abnormalities of pancreata of 8–10 month old G3 mTerc$^{-/-}$ mice compared to mTerc$^{+/+}$ mice (n = 75 mice per group, Figure 1A). In addition, we could not observe any change in pancreatic wet weight (7.615±0.5554 mg/g for mTerc+/+, 7.544±0.7685 mg/g for G3 mTerc$^{-/-}$ mice, p = 0.94, n = 6 each).

Despite normal appearing pancreatic histology, quantitative fluorescence in situ hybridisation (qFISH) revealed a marked reduction in telomere fluorescence intensity (TFI) in pancreata of G3 mTerc$^{-/-}$ mice (mean TFI: 2,103±102) compared to mTerc$^{+/+}$ mice (mean TFI: 4,683±277, p<0.0001, Figure 1B,C). Reductions in TFI are an established measure of telomere shortening [17].

Acute phase of cerulein-induced pancreatitis of telomerase knockout mice is similar to mTerc+/+ mice

It is not known, whether acute inflammatory conditions are altered in the context of telomere dysfunction. The peak stage of cerulein-induced pancreatitis occurs 9–12 h after the first cerulein injection. At this time point, the histological appearance of cerulein-induced pancreatitis (Figure 2A) and the histological scoring of pancreatits-associated inflammatory infiltrates, pancreatic edema, and necrosis (Figure 2B and Figure S1) revealed no difference in pancreata of 8-month-old G3 mTerc$^{-/-}$ mice compared to mTerc$^{+/+}$ mice (n = 5 mice per group). Similarly, the pancreatic wet weight, a measurement for pancreatits-induced edema, did not show significant differences between the two cohorts (Figure 2C). Moreover, lipase serum levels (a marker for acinar cell necrosis) did not reveal significant differences in cerulein-induced pancreatitis between the two cohorts (Figure 2D). TUNEL staining revealed similar rates of apoptosis in the pancreata of G3 mTerc$^{-/-}$ and mTerc$^{+/+}$ mice at the peak stage of cerulein-induced pancreatitis (Figure 2E,F). Together, these results indicated that telomere shortening did not change the severity of acute pancreatitis induced by repeated cerulein injection.

Regeneration after acute pancreatitis is impaired in telomerase knockout mice

In order to investigate the regeneration from acute cerulein-induced pancreatitis, pancreatic tissue of mTerc$^{+/+}$ and G3 mTerc$^{-/-}$ mice was examined 3 days and 7 days after pancreatitis induction. In the course of acute cerulein-induced pancreatitis, pancreata of 8-month-old mTerc$^{+/+}$ mice had almost completely regenerated after 3 days (Figure 3A,C). At this time point, age-

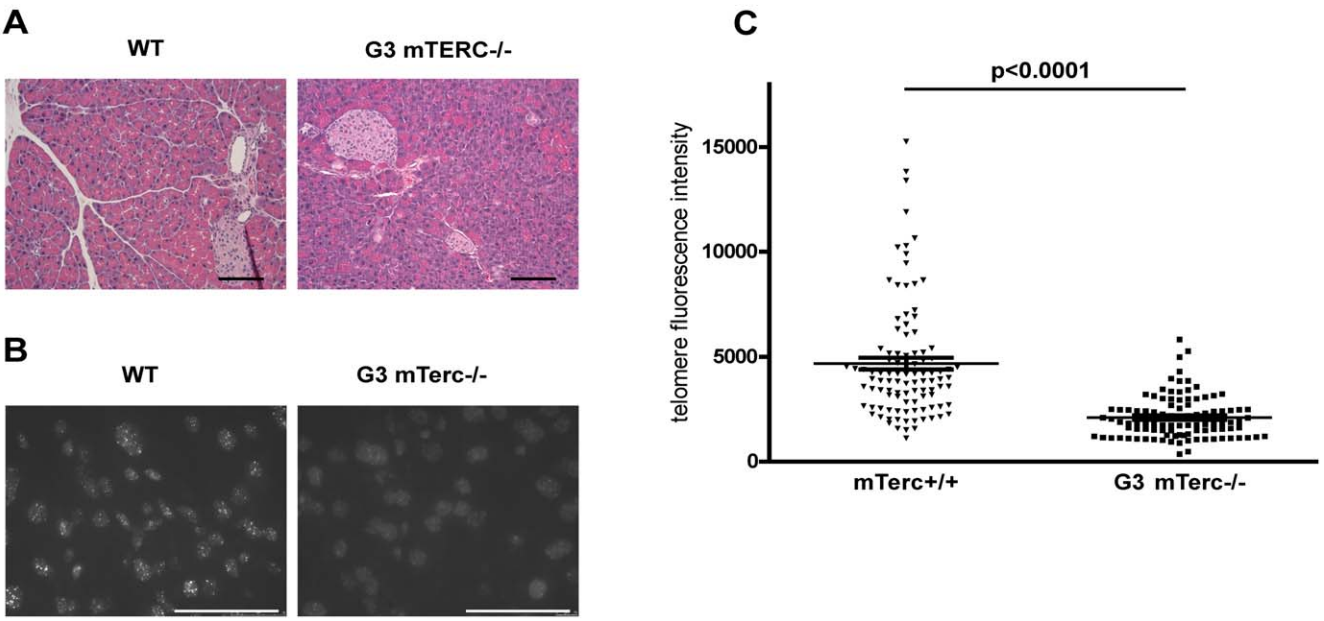

Figure 1. Normally developed pancreas despite shortened telomeres in telomerase knockout mice. (A) Representative H&E sections of mTerc$^{+/+}$ and G3 mTerc$^{-/-}$ mice reveal no differences in pancreas histology (size bar = 1 mm). (B) Telomere qFISH analysis reveals significantly decreased telomere fluorescence intensity in pancreata of G3 mTerc$^{-/-}$ compared to mTerc$^{+/+}$ mice (size bar = 50 μm). Depicted is an overlay of a representative DAPI (dark grey shaped nuclei) and corresponding telomere FISH signal (white dots; TFI = telomere fluorescence intensity). (C) Quantification of telomere fluorescence intensity. n = 5 mice per group; 20 nuclei per mouse were counted.
doi:10.1371/journal.pone.0017122.g001

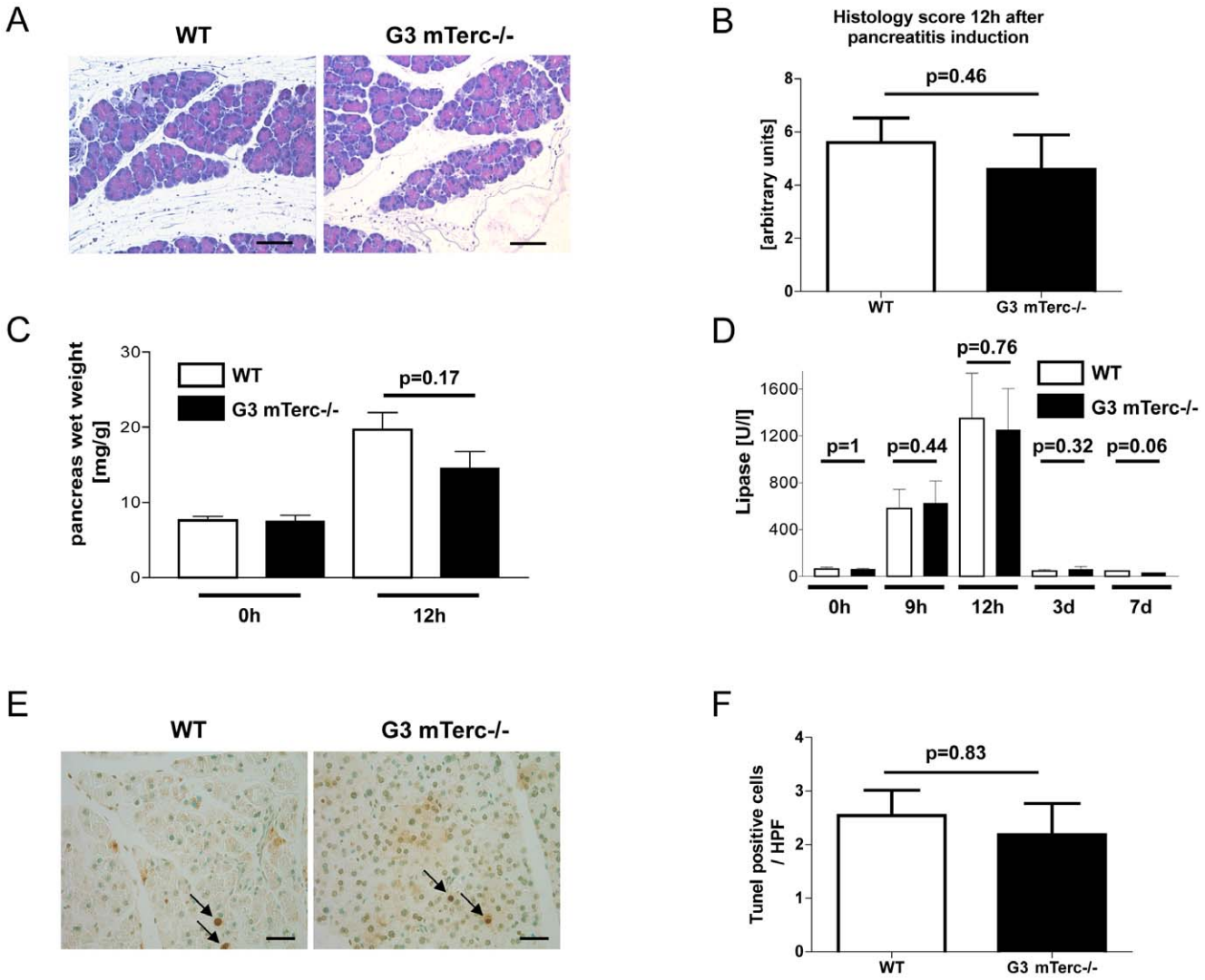

Figure 2. Acute pancreatitis in telomere-dysfunctional mice. (A) Representative H&E sections of indicated genotypes 12 h after pancreatitis induction (size bar = 500 μm). (B) Histological score of the indicated genotypes at 12 h after pancreatitis induction, n = 5 per group. The histological score is based on pancreatic edema, immune cell infiltration, and necrosis. (C) Pancreatic wet weight of mTerc$^{+/+}$ and G3 mTerc$^{-/-}$ mice at the indicated time points after pancreatitis induction. (D) Lipase serum levels of mTerc$^{+/+}$ and G3 mTerc$^{-/-}$ mice at the indicated time points after pancreatitis induction. (E) TUNEL staining of pancreata of indicated genotypes 12 h after pancreatitis induction (apoptotic cells are stained dark brown and marked with a black arrow; size bar = 200 μM) and its quantification (F), n = 5 per group. Error bars represent standard error mean (SEM).
doi:10.1371/journal.pone.0017122.g002

matched G3 mTerc$^{-/-}$ mice showed distinct areas of the exocrine pancreas with reduced eosin-positive cytoplasm and lack of apical zymogen granules. Moreover, these areas showed acinar to ductal metaplasia - a typical feature of cerulein-induced pancreatitis [18]. The metaplastic areas revealed a loss of amylase expression (Figure 3E,F and Figure S2A,B) and an expansion of ductal cells with formation of tubular complexes (Figure 3G,H and Figure S2C,D). A quantification of the amount of these metaplastic areas revealed a significant difference between the two cohorts 3 days after cerulein injection ($p = 0.048$; Figure 3K). In addition, Sirius red staining 3 days after pancreatitis induction revealed increased fibrosis in pancreata of G3 mTerc$^{-/-}$ mice compared to mTerc$^{+/+}$ mice (Figure 3I,J).

Apart from an increased occurrence of metaplastic tissue 3 days after pancreatitis induction, there were no signs of islet degeneration, evolution of diabetes mellitus, weight loss, or diarrhea upon 3-week-follow-up of G3 mTerc$^{-/-}$ mice. Histologically, the pancreata appeared normal on H&E staining after 3 weeks (Figure S3 and data not shown).

Furthermore, proliferating acinar cells were investigated by Ki-67 staining. No difference in proliferating acinar cells could be determined in un-stimulated pancreata of both groups (1.220 ± 0.4810 positive cells/high power field (HPF) $n = 6$ in mTerc+/+ and 1.175 ± 0.5921 positive cells/HPF $n = 4$ in G3 mTerc$^{-/-}$ mice, $p = 0.62$). In contrast, the proliferative response of acinar cell at day 3 after cerulein-induced pancreatitis was markedly reduced in G3 mTerc$^{-/-}$ mice (5.429 ± 2.241 Ki-67-positive cells per high power field, $n = 5$ mice) compared to mTerc$^{+/+}$ mice (33.43 ± 5.912 Ki-67 positive cells per high power field, $n = 5$, $p = 0.008$, Figure 4A,B). A similar impairment in pancreas regeneration of G3 mTerc$^{-/-}$ mice compared to mTerc$^{+/+}$ mice was seen at day 7 after cerulein-induced pancreatitis (Figure 4A, B). The Ki-67-positive acinar cells were evaluated in the non-metaplastic areas of the pancreas. In line with

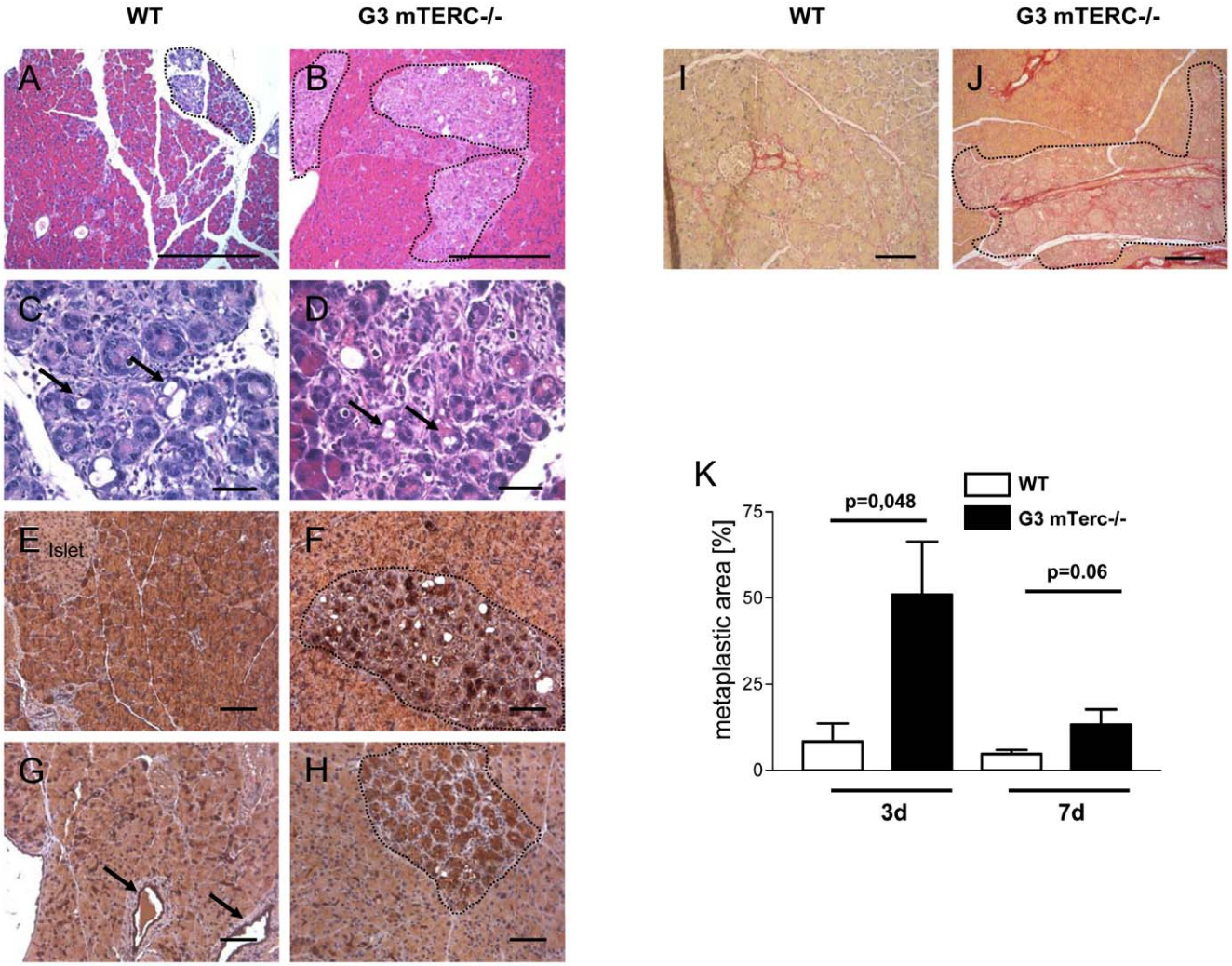

Figure 3. Impaired regeneration after acute pancreatitis in telomere-dysfunctional mice. Regeneration 3 d after induction of acute cerulein pancreatitis in mTerc$^{+/+}$ (A,C) and G3 mTerc$^{-/-}$ mice (B,D); arrows point to tubular complexes, degenerated area is encircled, H&E staining (A,B size bar = 1 mm; C,D size bar = 200 μm). De-differentiated tissue stains negative for amylase in G3 mTerc$^{-/-}$ mice (F) compared to mTerc$^{+/+}$ mice (E) with tubular complexes positive for CK-19 in mTerc$^{+/+}$ (G; arrows point to normal ducts) and G3 mTerc$^{-/-}$ mice (H; tubular complexes are in encircled area) (E-H size bar = 200 μm; amylase and CK-19 were stained with NovaRed (Vectorlabs) represented by red-brown color). Sirius red staining (stains fibrotic tissue red) reveals marked fibrosis in the de-differentiated tissue 3 d after pancreatitis induction in G3 mTerc$^{-/-}$ (J) compared to mTerc$^{+/+}$ mice (I; I,J size bar = 500 μm). (K) Quantification of the degenerated area in mTerc$^{+/+}$ and G3 mTerc$^{-/-}$ mice. Error bars represent SEM.
doi:10.1371/journal.pone.0017122.g003

the Ki-67 analysis on cell proliferation, mTerc$^{+/+}$ mice exhibited a stronger induction of proliferation markers characterizing the G2/M stage of the cell cycle (phospho-histone 3 (pH 3) and CDC2) compared to G3 mTerc$^{-/-}$ mice (Figure 4C).

DNA damage response in telomere-dysfunctional mice

In order to decipher possible mechanisms limiting pancreas regeneration in G3 mTerc$^{-/-}$ mice in response to cerulein-induced pancreatitis, mediators of the DNA damage response were analyzed in resting, non-injured pancreata (day 0) and in damaged pancreata (day 7 after cerulein application). Western blot analysis revealed an increased expression of p21 in resting, non-injured pancreata of G3 mTerc$^{-/-}$ mice compared to mTerc$^{+/+}$ mice. However, 7 days after cerulein-induced pancreatitis, no differences in the levels of activated p53 or p21 were observed in pancreata from G3 mTerc$^{-/-}$ mice compared to mTerc$^{+/+}$ mice (Figure 5). Phosphorylated Chk1 (an upstream kinase inducing DNA damage responses) was strongly expressed in non-injured pancreas of G3 mTerc$^{-/-}$ mice and mTerc$^{+/+}$ mice. In mTerc$^{+/+}$ mice, phospho-Chk1 expression declined during pancreas regeneration, whereas G3 mTerc$^{-/-}$ mice failed to inactivate phospho-Chk1 in response to pancreatic injury (Figure 5).

Discussion

The present study shows that pancreas regeneration in response to cerulein-induced pancreatitis is impaired in G3 mTerc$^{-/-}$ mice with shortened telomeres compared to mTerc$^{+/+}$ mice with longer telomere reserve. The experiments revealed no significant influence of telomere shortening on the severity of pancreatitis induced by cerulein injection. The severity of pancreatitis was evaluated histologically by lipase measurement and by pancreatic wet weight. In addition, TUNEL staining for evaluation of apoptosis that typically occurs in response to acute pancreatitis,

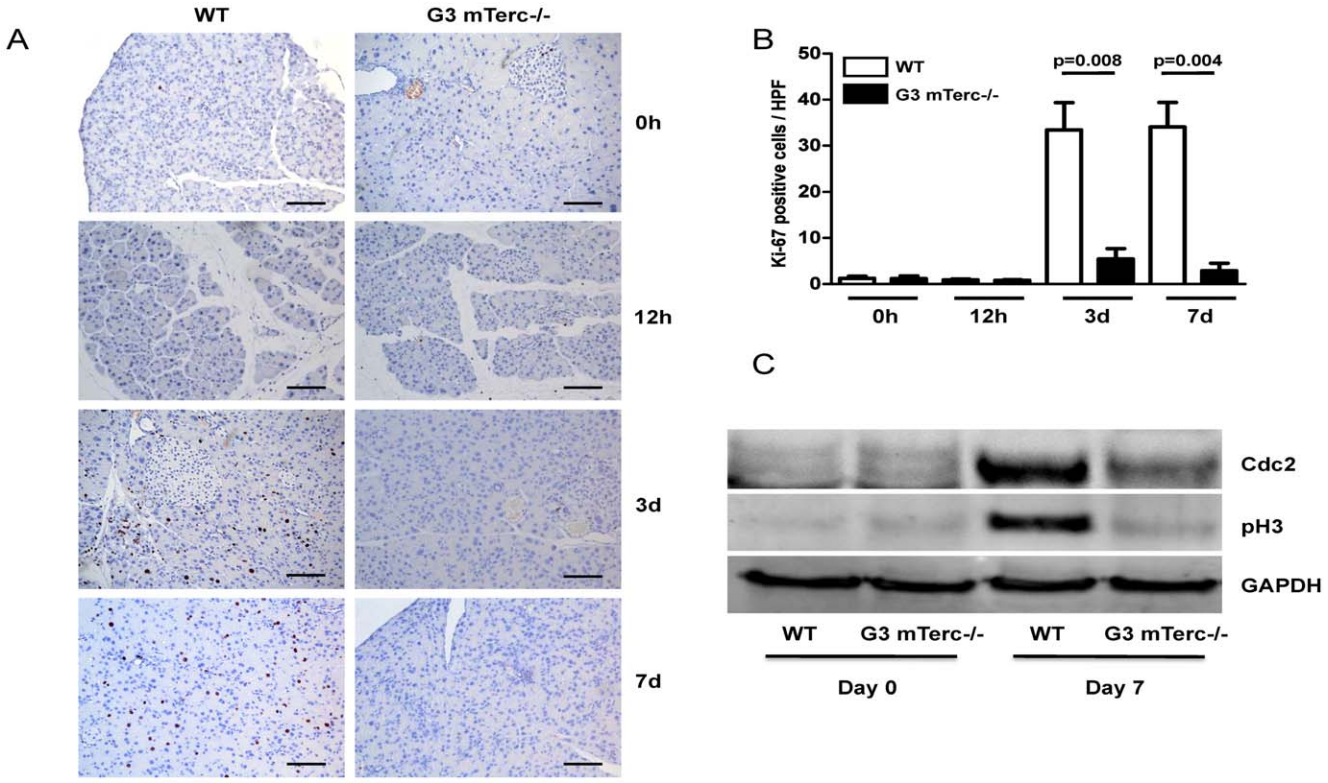

Figure 4. Block of proliferation in telomere-dysfunctional mice. (A) Representative pictures of Ki-67 staining of pancreata of indicated genotype and time point after pancreatitis (Ki-67 positive nuclei are stained black; size bar = 500 μm). (B) Quantification of Ki-67 positive cells of mTerc$^{+/+}$ and G3 mTerc$^{-/-}$ mice at indicated time points after pancreatitis induction. (C) Analysis of cell cycle proteins in pancreata of mTerc$^{+/+}$ and G3 mTerc$^{-/-}$ mice before and 7 d after pancreatitis induction (pH3 = phospho Histone 3 Serine 10).
doi:10.1371/journal.pone.0017122.g004

was performed. Together, these data showed no changes between G3 mTerc$^{-/-}$ compared to mTerc$^{+/+}$ mice indicating that differences in the regenerative response were not due to differences in the initiated levels of tissue damage.

The delay in pancreatic regeneration in the context of telomere shortening was associated with the persistence of metaplastic exocrine tissue, the formation of tubular complexes, and an increase in fibrotic tissue at 3 days after tissue injury. Increased pancreatic fibrosis and tubular complexes are also a hallmark of human chronic pancreatitis [19,20]. Based on our study, it should be evaluated whether telomere shortening correlates with the development of fibrosis and tubular complexes in patients with chronic pancreatitis. However, up to now it is not known, whether telomere shortening can be observed in the evolution of human chronic pancreatitis.

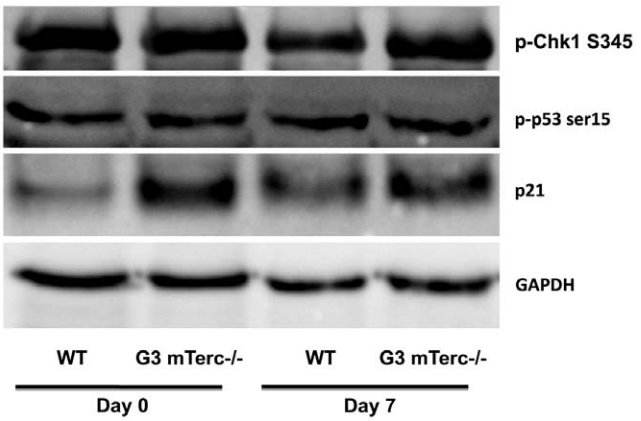

Figure 5. DNA damage response protein expression during regeneration of the pancreas. pChk1, p53 and p21 expression in pancreata of mTerc$^{+/+}$ and G3 mTerc$^{-/-}$ mice before and 7 d after pancreatitis induction.
doi:10.1371/journal.pone.0017122.g005

Delayed pancreas regeneration was found to be associated with impaired proliferation rates in pancreata of cerulein-treated G3 mTerc$^{-/-}$ mice compared to mTerc$^{+/+}$ mice. Previous studies have revealed that proliferating cells seen after acute cerulein-induced pancreatitis are mainly differentiated acinar cells that contribute to tissue repair [21]. Studies on telomerase knockout mice have shown that telomere shortening affects stem cell compartments of highly proliferative organs and impairs regeneration of somatic tissues by activating p21-dependent cell cycle arrest [22]. In contrast, the current study did not reveal a pronounced induction of p53 or p21 in pancreata of G3 mTerc$^{-/-}$ compared to mTerc+/+ mice. However, G3 mTerc$^{-/-}$ mice showed an impaired inactivation of phospho-Chk1 in response to pancreas injury compared to mTerc$^{+/+}$ mice. These data suggest that p53-independent pathways contribute to impairments in pancreas regeneration in response to telomere shortening possibly involving Chk1.

It has been shown that transient dedifferentiation and proliferation of acinar cells is required for exocrine pancreas regeneration after cerulein damage [21,23]. It is conceivable that impaired acinar cell regeneration led to delayed pancreas

regeneration and a prolonged persistence of metaplastic tissue in the pancreata of G3 mTerc$^{-/-}$ mice compared to mTerc$^{+/+}$ mice. However, G3 mTerc$^{-/-}$ mice did not fail to complete pancreas regeneration, the process was just delayed. It remains to be investigated whether a delay in pancreas regeneration could lead to manifest pancreas defects in the context of chronic organ damage. If so, telomere shortening could represent a causal factor influencing disease progression in chronic pancreatitis.

In summary, this study presents the first experimental evidence that the induction of acute pancreatitis by cerulein treatment is not altered by telomere shortening in mice. However, telomere shortening was associated with delayed regeneration after acute pancreatitis apparently involving p53- and p21-independent mechanisms.

Materials and Methods

Animal experiments

mTerc+/+ and mTerc$^{-/-}$ mice were held in a pathogen-free area (20–22°C) with free access to food and water.

For the induction of pancreatitis, mice were starved for 18 h and injected 6 hourly doses of 100 µg/kg cerulein (Takus, Pfizer) i.p. Mice were sacrificed at the indicated time points after the first injection of cerulein.

The animal experiments were approved by the government of the state of Baden-Württemberg (animal protocol number 35/915.81-3/919).

Histology score

The histology score was calculated blindly by M.W. The score is based on the level of pancreatic edema, immune cell infiltrate, and acinar cell necrosis and was determined as previously described [24].

qFISH analysis for telomere length

Telomere length was determined on 5 µm-thick paraffin sections using quantitative fluorescence in situ hybridization (qFISH) according to previously reported methods [25]. Briefly, unmasked sections were incubated in pepsine solution (200 mg pepsine, 168 µl HCL 37%, up to 200 ml H_2O) for 6 min at 37°C. After washing with phosphate-buffered saline, slides were hybridized with hybridization mix (10 mmol/L Tris pH 7.2; MgCl2 buffer: 7.02 mmol/L Na2HPO3, 2.14 mmol/L MgCl2, 0.77 mmol/L citric acid; 70% deionized formamide; 0.5 µg/mL PNA probe 5-Cy3-CCC TAA CCC TAA CCC TAA-3 Applied Biosystems; 0.25% blocking reagent from Roche) at 80°C for 3 min followed by a 2 h incubation at RT. After washing with formamide solution (70 ml formamide, 1 ml 1 M Tris pH7,2, 1 ml BSA 10%, up to 100 ml H_2O) and phosphate-buffered saline, sections were mounted with DAPI. The relative telomere length was determined by quantification of the fluorescence intensity using TFL software [17].

Lipase measurement

Lipase was measured in serum of the mice in the clinical chemistry department of the University Hospital of Ulm with the same protocol and equipment as for routine measurement of human samples. Before measurement, the serum was diluted 1:4 with PBS.

Immunohistochemistry

H&E staining was performed according to standard procedures. Quantification of degenerated tissue was performed on serial pictures of H&E-stained pancreatic tissue (50x magnification; 10 pictures per pancreas) by determination of the degenerated area using Image J software. The degenerated area was identified by lack of eosin-positive cytoplasm and disturbed tissue integrity on H&E-stained sections. These areas were encircled and quantified using ImageJ (an example is shown in Figure 3A,B).

Immunofluorescence was performed on paraffin-embedded pancreas using primary anti-amylase (Santa Cruz) and anti-CK19 (Santa Cruz). Ki-67 immunohistochemistry was performed on paraffin-embedded pancreas using primary anti-Ki67 (Monosan). Primary and secondary antibody dilutions were 1:200 and 1:250, respectively. Immunohistochemistry was performed on paraffin-embedded pancreas using primary anti-amylase (Santa Cruz) and anti-CK19 (Santa Cruz). Primary and secondary antibody dilutions were 1:100 and 1:200, respectively. For development ABC Kit (Vector labs) and NovaRed peroxidase substrate kit (Vector labs) was used. TUNEL staining was performed according to the manufacturer's protocol (Roche). Sirius Red staining was performed according to standard procedures. Sirius red stains fibrotic tissue red. The metaplastic areas were identified on Sirius red-stained slides by disturbed tissue morphology and lack of yellow-stained cytoplasm. For amylase and CK19 staining, at least 3–5 mice per time point and per genotype were stained and representative pictures were taken. For Ki-67 staining, non-metaplastic areas of the pancreas were evaluated since the metaplastic areas are infiltrated by many immune cells that proliferate and do not represent proliferation of acinar cells. The magnification of the evaluated pictures was 200x and the Ki67-positive cells per picture was determined.

Immunoblot analysis

Whole-cell extracts were prepared according to standard protocols and tested by western blot using anti-P21 (Santa Cruz), anti-pP53 (Cell Signalling), anti-pChk1 (Cell Signalling), anti-Cdc2 (Santa Cruz), anti-pH3 (Santa Cruz), and anti-GAPDH (Bethyl laboratory). Dilutions of the primary and secondary antibodies were 1:1,000 1:10,000, respectively. Western blots were performed on pooled samples of n = 3–5 pancreata per time point and genotype.

Blood sugar measurement

Blood sugar was measured using a glucometer (OneTouch Ultra) by withdrawing blood from the tail vene of non-starved mice in the afternoon.

Statistical analysis

Statistical analysis was performed with GraphPad Prism using rank-based Mann-Whitney test.

Supporting Information

Figure S1 Histological score in acute pancreatitis. Histological score of the indicated genotypes at 12 h after pancreatitis induction, n = 5 per group. The histological score is depicted separately for (A) pancreatic edema (p = 0.55), (B) immune cell infiltration (p = 0.42), and (C) necrosis (p = 0.69).
(TIF)

Figure S2 Metaplastic tissue after acute pancreatitis in telomere-dysfunctional mice. Metaplastic tissue 3 d after induction of acute cerulein pancreatitis in mTerc$^{+/+}$ and G3 mTerc$^{-/-}$ mice was analyzed by amlylase (A,B) and CK-19 staining (C,D; A-D size bar = 100 µm). De-differentiated tissue (encircled area) stains negative for amylase in G3 mTerc$^{-/-}$ mice (B) compared to mTerc$^{+/+}$ mice (A) with tubular complexes (arrows) positive for CK-19 in mTerc$^{+/+}$ (C) and G3 mTerc$^{-/-}$ mice (D). Fluorescence staining: amylase = red, DAPI = blue, CK-19 = red, DAPI = blue.
(TIF)

Figure S3 Blood sugar and body weights are stable after induction of acute pancreatitis. Acute pancreatitis was induced using cerulein in mTerc$^{+/+}$ (n = 7) and G3 mTerc$^{-/-}$ (n = 7) mice. The indicated genotypes were followed over 3 weeks measuring body weight (A) and blood sugar (B) at the given time points.
(TIF)

Author Contributions

Conceived and designed the experiments: KLR GvF. Performed the experiments: GvF MW KN. Analyzed the data: GvF KLR MW DH AK LMG. Contributed reagents/materials/analysis tools: KLR GvF MW HR. Wrote the paper: GvF KLR. Critically read and contributed to manuscript preparation: GA.

References

1. Levy MZ, Allsopp RC, Futcher AB, Greider CW, Harley CB (1992) Telomere end-replication problem and cell aging. J Mol Biol 225(4): 951–960.
2. Lee HW, Blasco MA, Gottlieb GJ, Horner JW, 2nd, Greider CW, et al. (1998) Essential role of mouse telomerase in highly proliferative organs. Nature 392(6676): 569–574.
3. Choudhury AR, Ju Z, Djojosubroto MW, Schienke A, Lechel A, et al. (2007) Cdkn1a deletion improves stem cell function and lifespan of mice with dysfunctional telomeres without accelerating cancer formation. Nat Genet 39(1): 99–105.
4. Wright WE, Shay JW (1992) The two-stage mechanism controlling cellular senescence and immortalization. Exp Gerontol 27(4): 383–389.
5. Brown JP, Wei W, Sedivy JM (1997) Bypass of senescence after disruption of p21CIP1/WAF1 gene in normal diploid human fibroblasts. Science 277(5327): 831–834.
6. Jiang H, Ju Z, Rudolph KL (2007) Telomere shortening and ageing Z. Gerontol Geriatr 40(5): 314–324.
7. Armanios MY, Chen JJ, Cogan JD, Alder JK, Ingersoll RG, et al. (2007) Telomerase mutations in families with idiopathic pulmonary fibrosis. N Engl J Med 356(13): 1317–1326.
8. Mitchell JR, Wood E, Collins K (1999) A telomerase component is defective in the human disease dyskeratosis congenita. Nature 402(6761): 551–555.
9. Wiemann SU, Satyanarayana A, Tsahuridu M, Tillmann HL, Zender L, et al. (2002) Hepatocyte telomere shortening and senescence are general markers of human liver cirrhosis. FASEB J 16(9): 935–942.
10. Blasco MA, Lee HW, Hande MP, Samper E, Lansdorp PM, et al. (1997) Telomere shortening and tumor formation by mouse cells lacking telomerase. RNA Cell 91(1): 25–34.
11. Rudolph KL, Chang S, Lee HW, Blasco M, Gottlieb GJ, et al. (1999) Longevity, stress response, and cancer in aging telomerase-deficient mice. Cell 96(5): 701–712.
12. Rudolph KL, Chang S, Millard M, Schreiber-Agus N, DePinho RA (2000) Inhibition of experimental liver cirrhosis in mice by telomerase gene delivery. Science 287(5456): 1253–1258.
13. Satyanarayana A, Geffers R, Manns MP, Buer J, Rudolph KL (2004) Gene expression profile at the G1/S transition of liver regeneration after partial hepatectomy in mice. Cell Cycle 3(11): 1405–1417.
14. Gardner TB, Vege SS, Chari ST, Pearson RK, Clain JE, et al. (2008) The effect of age on hospital outcomes in severe acute pancreatitis. Pancreatology 8(3): 265–270.
15. Ishii A, Nakamura K, Kishimoto H, Honma N, Aida J, et al. (2006) Telomere shortening with aging in the human pancreas. Exp Gerontol 41(9): 882–886.
16. Willemer S, Elsasser HP, Adler G (1992) Hormone-induced pancreatitis. Eur Surg Res 24(Suppl 1): 29–39.
17. Poon SS, Martens UM, Ward RK, Lansdorp PM (1999) Telomere length measurements using digital fluorescence microscopy Cytometry 36(4): 267–278.
18. Willemer S, Elsasser HP, Kern HF, Adler G (1987) Tubular complexes in cerulein- and oleic acid-induced pancreatitis in rats: Glycoconjugate pattern, immunocytochemical, and ultrastructural findings. Pancreas 2(6): 669–675.
19. Bockman DE, Boydston WR, Anderson MC (1982) Origin of tubular complexes in human chronic pancreatitis. Am J Surg 144(2): 243–249.
20. Witt H, Apte MV, Keim V, Wilson JS (2007) Chronic pancreatitis: Challenges and advances in pathogenesis, genetics, diagnosis, and therapy. Gastroenterology 132(4): 1557–1573.
21. Elsasser HP, Adler G, Kern HF (1986) Time course and cellular source of pancreatic regeneration following acute pancreatitis in the rat. Pancreas 1(5): 421–429.
22. Satyanarayana A, Wiemann SU, Buer J, Lauber J, Dittmar KE, et al. (2003) Telomere shortening impairs organ regeneration by inhibiting cell cycle re-entry of a subpopulation of cells. EMBO J 22(15): 4003–4013.
23. De Lisle RC, Grendell JH, Williams JA (1990) Growing pancreatic acinar cells (postpancreatitis and fetal) express a ductal antigen. Pancreas 5(4): 381–8.
24. Rongione AJ, Kusske AM, Kwan K, Ashley SW, Reber HA, et al. (1997) Interleukin 10 reduces the severity of acute pancreatitis in rats. Gastroenterology 112(3): 960–967.
25. Lechel A, Holstege H, Begus Y, Schienke A, Kamino K, et al. (2007) Telomerase deletion limits progression of p53-mutant hepatocellular carcinoma with short telomeres in chronic liver disease. Gastroenterology 132(4): 1465–1475.